Angewandte Chemie

Eine Zeitschrift der Gesellschaft Deutscher Chemiker

www.angewandte.de

Akzeptierter Artikel

Titel: Click-Chemistry-Mediated Cell Membrane Glycopolymer Engineering to Potentiate Dendritic Cell Vaccines

Autoren: He Yang, Zijian Xiong, Xingyu Heng, Xiaomeng Niu, Yichen Wang, Lihua Yao, Lele Sun, Zhuang Liu, and Hong Chen

Zitierweise: *Angew. Chem. Int. Ed.* **2023**, e202315782

Link zur VoR: https://doi.org/10.1002/anie.202315782

WILEY VCH

10.1002/ange.202315782

WILEY VCH

RESEARCH ARTICLE

Click-Chemistry-Mediated Cell Membrane Glycopolymer Engineering to Potentiate Dendritic Cell Vaccines

He Yang,[a] Zijian Xiong,[b] Xingyu Heng,[a] Xiaomeng Niu,[a] Yichen Wang,[a] Lihua Yao,[a] Lele Sun,*[c] Zhuang Liu*[b] and Hong Chen*[a]

[a] H. Yang, X. Heng, X. Niu, Y, Wang, L. Yao, Prof. Dr. H, Chen
College of Chemistry, Chemical Engineering and Materials Science
Soochow University
Suzhou, 215123, Jiangsu (China)
E-mail: chenh@suda.edu.cn

[b] Z. Xiong, Prof. Dr. Z. Liu
Institute of Functional Nano & Soft Materials (FUNSOM)
Jiangsu Key Lab Carbon Based Functional Materials and Devices
Soochow University
Suzhou, 215123, Jiangsu (China)
Email: zliu@suda.edu.cn

[c] Prof. Dr. L. Sun
Institute of Materiobiology, Department of Chemistry, College of Science
Shanghai University
Shanghai, 200444 (China)
Email: sunlele@shu.edu.cn

Supporting information for this article is given via a link at the end of the document.

Abstract: Dendritic cell vaccine (DCV) holds great potential in tumor immunotherapy owing to its potent ability in eliciting tumor-specific immune responses. Aiming at engineering enhanced DCV, we report the first effort to construct a glycopolymer-engineered DC vaccine (G-DCV) via metabolic cell surface sugar engineering and copper-free click-chemistry. Model G-DCV was prepared by firstly delivering tumor antigens, ovalbumin (OVA) into dendritic cells (DC) with fluoroalkane-grafted polyethyleneimines, followed by conjugating glycopolymers with a terminal group of dibenzocyclooctyne (DBCO) onto dendritic cells. Compared to unmodified DCV, our G-DCV could induce stronger T cell activation due to the enhanced adhesion between DCs and T cells. Notably, such G-DCV could more effectively inhibit the growth of the mouse B16-OVA (expressing OVA antigen) tumor model after adoptive transfer. Moreover, by combination with an immune checkpoint inhibitor, G-DCV shows further increased anti-tumor effects in treating different tumor models. Thus, our work provides a novel strategy to enhance the therapeutic effectiveness of DC vaccines.

Introduction

Dendritic cells (DC) are critical for initiating antigen-specific T cell activation in adaptive immunity[1]. Therefore, dendritic cell-based tumor vaccines which eliminate tumors in an antigen-specific manner have been considered to be one of the most promising strategies for tumor immunotherapy[2]. However, although DC vaccines have been tested in patients with malignant melanoma, prostate cancer, malignant glioma, and renal cell cancer[3], their therapeutic efficacy remains limited in the clinic. The efficient recognition and binding of T cell receptor (TCR) on the surface of T cells by peptide-major histocompatibility complex (pMHC) is critical for DCs to activate antigen-specific T cells[4]. Therefore, various methods, such as modifying the tumor antigens with DCs targeting molecules, and constructing more efficient antigen delivery carriers as well as adjuvants, have been proposed to improve the therapeutic efficacy of DC vaccines by promoting antigen presentation of DCs[5]. For instance, Dhodapkar et al. modified the tumor antigens with monoclonal antibodies which could target DCs to enhance the antigen presentation[5b]. Xu et al. reported a novel antigen carrier, fluoroalkane-grafted polyethyleneimines (F-PEI), with an efficient antigen cross-presentation[5c]. Previous research has demonstrated that DC-T cell adhesion also plays a pivotal role in T cell activation by promoting the formation of immune synapses and subsequent pMHC-TCR recognition[6]. Therefore, in addition to increasing the density of antigens presented on DCs, enhancing the adhesion between DCs and T cells is also promising in augmenting the therapeutic efficacy of DC vaccine (DCV).

Among the numerous adhesion molecules, carbohydrate-lectin binding, due to its stability and specificity, plays an important role in intercellular adhesion, cell targeting, and recognition[7]. Recently, researchers have explored the strategy to regulate cell behavior by artificially modifying glycan on the cell surface[7b, 7d, 8]. For instance, the modification of mesenchymal stem cells with sialyl Lewis X through biotin-avidin interaction resulted in enhanced rolling response and homing effect to inflamed

10.1002/ange.202315782

RESEARCH ARTICLE

tissues[7b]. Our group demonstrated that glycopolymer-engineered Hela cells induced an improved phagocytic response with macrophages[8]. Moreover, in our previous study, we employed the DC2.4 cell line as a model to generate glycopolymer-engineered DCs via tag protein fusion technique, and the glycopolymer-engineered DCs facilitated T cell activation by augmenting intercellular adhesion[7d]. However, the tag protein fusion approach for constructing glycopolymer-engineered DCs is not applicable for primary DCs due to the sophisticated procedure, as well as the damage caused by the gene transfection process to primary cells[9]. In addition, the strong immunogenicity of the exogenous protein tag could induce antibody production, which might lead to immune clearance of DC vaccines.

In recent years, copper-free click-chemistry combined with metabolic sugar engineering has been widely used to modify the surface protein of cells with diverse molecules [10]. Such a method provides a powerful platform for the covalent modification of cell surface with long retention time as well as low cytotoxicity[11]. Therefore, in this study, to enhance the effectiveness of DC vaccines, we applied this method to equip DCs with glycopolymers to promote the adhesion between DCs and T cells (**Figure 1**). Glycopolymers with dibenzocyclooctyne (DBCO) terminal groups were synthesized via reversible addition-fragmentation chain transfer (RAFT) polymerization and terminal group transition, and then modified onto primary DCs utilizing copper-free click-chemistry in combination with metabolic sugar engineering to construct glycopolymer-engineered DC vaccine (G-DCV). It was observed that the glycopolymers on DCs surface could effectively enhance the adhesion between G-DCV and T cells, and the enhanced adhesion effects were increased with the surface glycopolymer density until the plateau. T cell activation assays showed that compared to unmodified DCV, G-DCV could activate and expand T cells more effectively both in vitro and in vivo. Adoptive transfer of G-DCV showed an effective anti-tumor effect on B16-OVA (expressing OVA antigen) tumor models. Further combined with immune checkpoint inhibitors, G-DCV could more effectively inhibit tumor growth in both B16-OVA and CT-26 tumor models. Therefore, the present work demonstrated that glycopolymer engineering would be a new idea to potentiate DC vaccines.

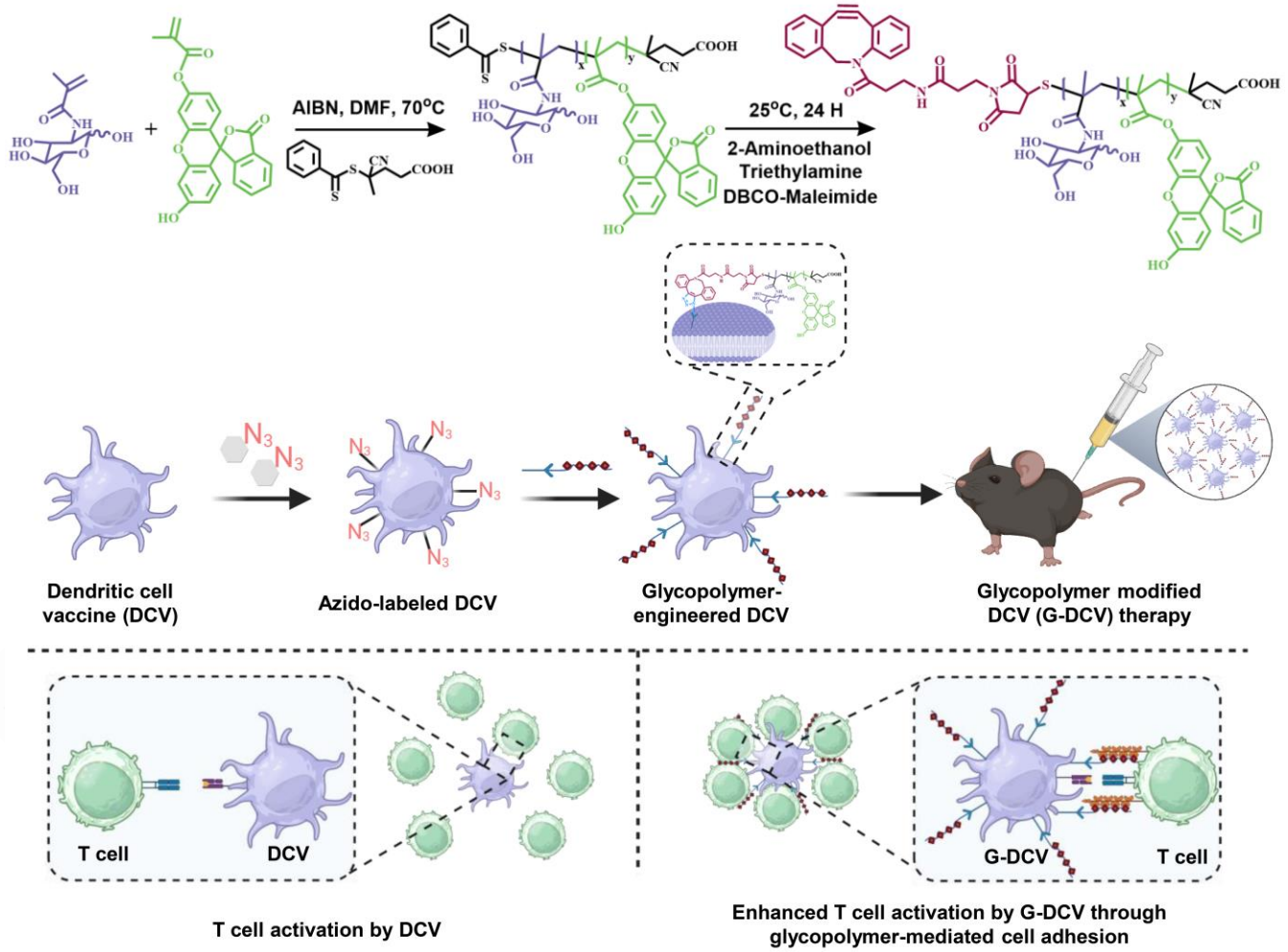

Figure 1. Schematic diagram of construction and application of glycopolymer-engineered DC vaccines. The prepared DC vaccines were modified with glycopolymers via coper-free click-chemistry in combination with metabolic sugar engineering; G-DCV facilitates the adhesion of dendritic cells to T cells employing glycopolymers, thereby augmenting T cell activation.

10.1002/ange.202315782

Results and Discussion

Construction and characterization of G-DCV

G-DCV was constructed as illustrated in **Figure 2A**. The immature bone marrow-derived dendritic cells (BMDCs) were initially incubated with tetraacetyl-*N*-azidoacetylmannosamine ($Ac_4ManNAz$) for 3 days to obtain the azido-labeled DCs. On the third day of the azido-labeling process, an existing method was adapted to generate DCV by delivering the model antigen ovalbumin (OVA) into DCs using fluoroalkane-grafted polyethyleneimine (F-PEI) as delivery carrier[5c, 12]. Subsequently, glycopolymers were covalently modified on the surface of the azido-labeled DCs resulting in the construction of G-DCV.

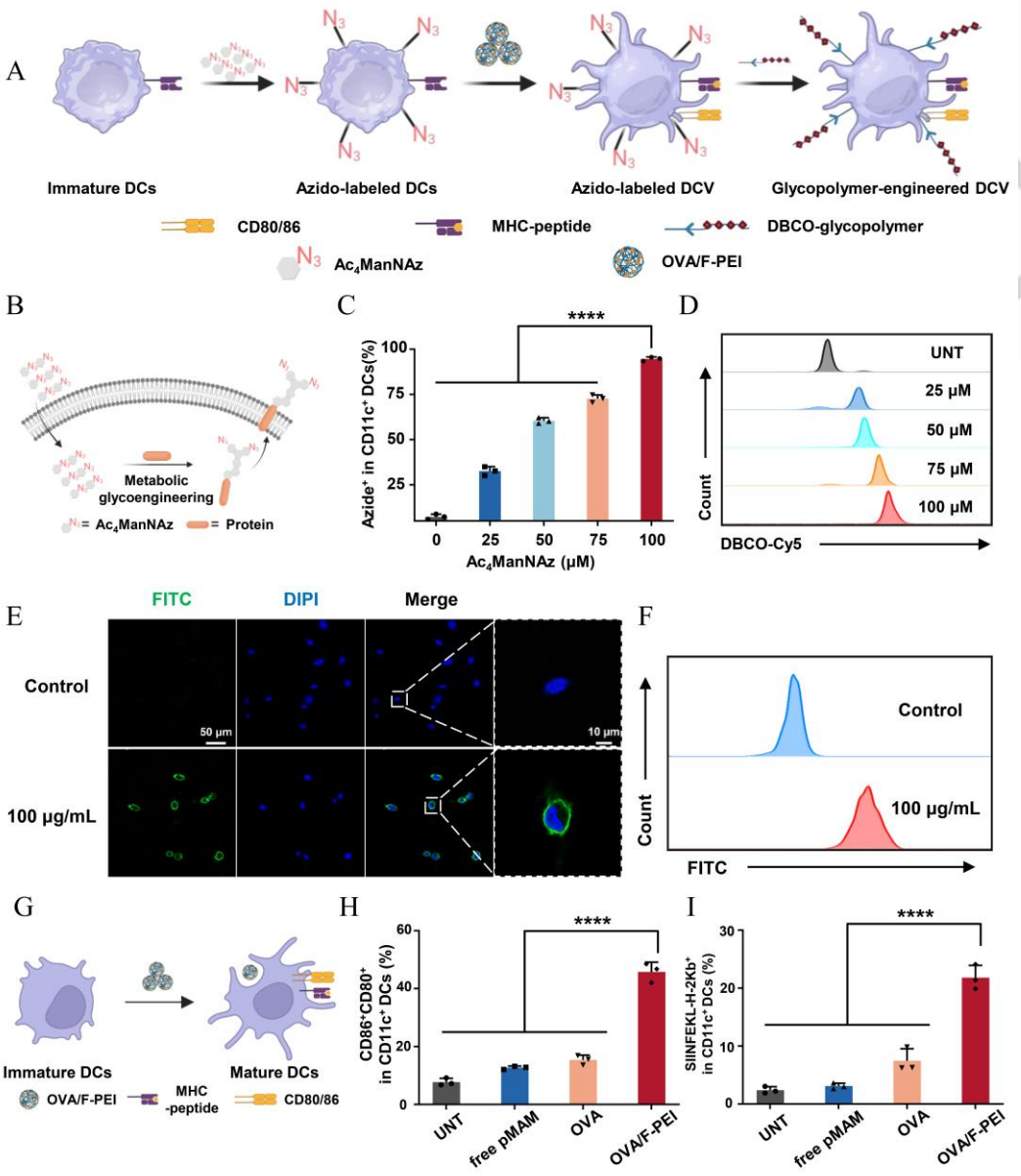

Figure 2. Preparation of glycopolymer-engineered DC vaccines. (A) Schematic diagram of the construction of the G-DCV; (B) Schematic diagram of metabolic labeling of DCs with $Ac_4ManNAz$; (C) Percentage of azido$^+$ BMDCs after 3 days of incubation with different concentrations of $Ac_4ManNAz$; (D) Flow cytometry data showing azido groups on BMDCs under various concentrations of $Ac_4ManNAz$. Azido groups on the BMDCs surface were detected by DBCO-Cy5; (E) Confocal images of DCs after 3 days of incubation with $Ac_4ManNAz$ and 30 minutes staining with different concentrations of glycopolymer-DBCO; (F) Flow cytometry data showing glycopolymer modified on BMDCs under various concentrations; (G) Schematic diagram of the preparation of the DC vaccines; (H) Statistical data showing $CD80^+CD86^+$and (I) OVA antigen cross-presentation in BMDCs treated with PBS, pMAM, OVA, and OVA/F-PEI for 12 hours. The error bars represent mean ± SD (n = 3). Statistical analysis was performed using Tukey's multiple comparison test and, ****$p < 0.0001$.

Specifically, we synthesized glycopolymers, poly-mannose (pMAM), via RAFT polymerization using 2-methacrylamido mannose as the monomer and 4-cyanopentanoic acid dithiobenzoate (CPADB) as the chain transfer agent. The terminal thiol group after deprotection was conjugated with DBCO-maleimide[13] (**Figure S1, 2**). Fluorescein O-methacrylate (FluMA), the fluorescent co-monomer, was also utilized in the polymerization as a fluorescent marker and was characterized by fluorescence spectroscopy (**Figure S3 and Table S1**).

Next, we used $Ac_4ManNAz$, a commonly used live cell metabolic labeling agent, to label BMDCs (**Figure 2B**). After incubating BMDCs with varying concentrations of $Ac_4ManNAz$ for

10.1002/ange.202315782

3 days, those cells were metabolically labeled in a concentration-dependent manner, with over 90% of cells labeled with azido when the concentration of Ac_4ManNAz reached 100 μM (**Figure 2C, D**). Meanwhile, our experimental results indicated that Ac_4ManNAz exhibited no significant cytotoxicity within the tested concentration range (**Figure S4**). Therefore, a concentration of 100 μM Ac_4ManNAz was selected in subsequent experiments.

Afterwards, the surface glycopolymer-covalent modification of DCs was performed by incubating glycopolymer-DBCO with azido-group-expressing DC vaccines. Confocal images showed that glycopolymers with fluorescent monomers were modified on the surface of dendritic cells and could remain on the DCs for more than 48 hours, which is enough for T cell activation based on the previous study[14] (**Figure 2E, S5**). The success of glycopolymer modification was also proved by flow cytometry results (**Figure 2F**). Furthermore, the density of glycopolymers on the surface of DCs could be regulated by adjusting the quantity of glycopolymer-DBCO used during the modification process (**Fig. S6, 7**).

The antigen presented by matured DCs is critical for the activation of $CD8^+$ T cells and subsequent anti-tumor immune responses[15]. In this study, OVA/F-PEI nanoparticles (OVA/F-PEI NPs) were employed to establish a model DCV with a certain degree of maturation and antigen cross-presentation due to the high efficiency of antigen delivery and cell compatibility[5c] (**Figure 2G**). OVA was mixed with F-PEI at a 1:1 weight ratio (pH=7.0) to form OVA/F-PEI NPs with a hydrodynamic size at around 130 nm and zeta potential at around +46 mV (**Figure S8** and **Table S2**). The transmission electron microscope (TEM) image of the nanoparticles revealed a size comparable to that determined by dynamic light scattering (DLS) (**Figure S9**). After incubating BMDCs with Ac_4ManNAz for 60 hours, OVA/F-PEI nanoparticles were introduced to the co-incubation environment for an additional 12 hours. The flow cytometry results revealed a notable increase in the percentage of matured DCs characterized by $CD80^+CD86^+$ expression, rising from 7.7% to 45.8% (**Figure 2H**). Previous studies demonstrated that treatment with Ac_4ManNAz or some glycans could facilitate DC maturation[16]. However, the observed promotion was not significant in our experimental system (**Figure S10**). In addition, the CD80 and CD86 levels of DCV (BMDCs only treated with F-PEI/OVA) and G-DCV (BMDCs treated with F-PEI/OVA, Ac_4ManNAz and glycopolymer-DBCO), but no significant differences were observed, which might be attributed to the dominant role played by F-PEI/OVA in promoting DC maturation in our experimental model (**Figure S10**). Furthermore, the presentation of SIINFEKL peptides on the surface of BMDCs showed an almost three-fold improvement compared to the free antigen treatment group (**Figure 2I**). Therefore, we successfully constructed the glycopolymer-engineered DC vaccines with controllable glycopolymer density.

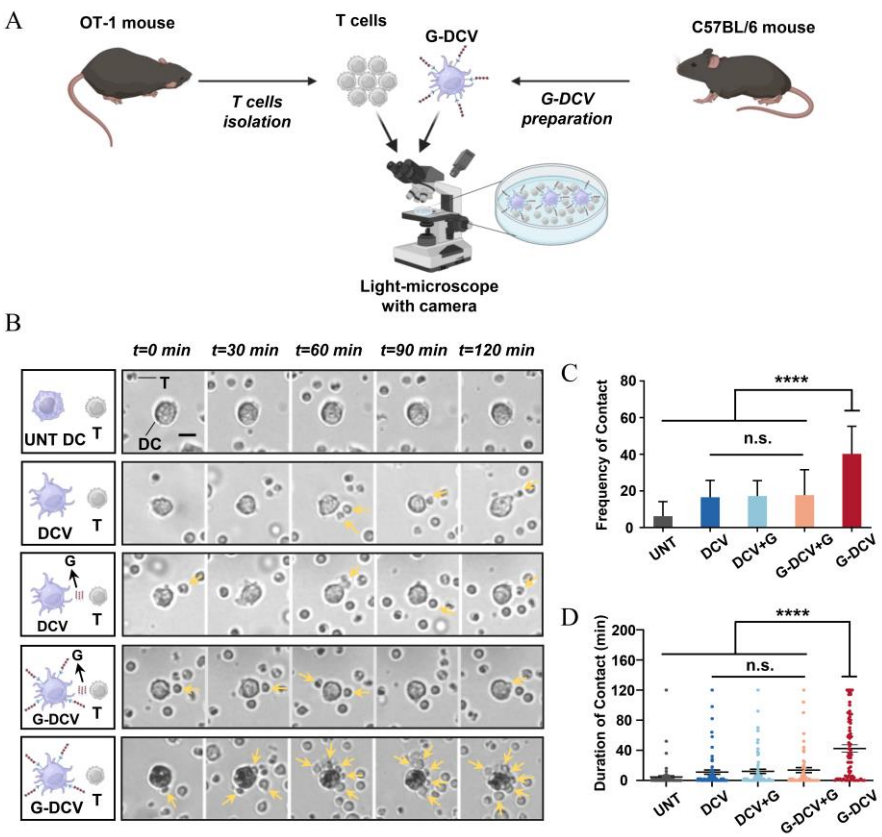

Figure 3. Investigation of adhesion behavior between G-DCV and T cells. (A) Schematic diagram of cell image tracking experiment. T cells were incubated with DCV at a ratio of 10:1; (B) Image tracking of BMDCs and T cells migration over time. "G": glycopolymers. The scale bar is 10 μm; (C) Frequency of contact between BMDCs and T cells; (D) Duration of contact between BMDCs and T cell, with T cell number (n= 70). UNT: untreated immature BMDCs; DCV: mature BMDCs; DCV+G: mature BMDCs and free glycopolymers in the cell culture medium; G-DCV+G: mature BMDCs modified with glycopolymers and free glycopolymers in the cell culture medium; G-DCV: mature BMDCs modified with glycopolymers. The error bars represent mean ± SD (n = 70). Statistical analysis was performed using Tukey's multiple comparison test and, ****$p < 0.0001$.

10.1002/ange.202315782

RESEARCH ARTICLE

Investigation of adhesion behavior between G-DCV and T cells

The adhesion between DCs and T cells plays a crucial role during the early stages of T cell activation, as indicated by previous research[6, 7d]. We then employed a cell image tracking experiment to determine whether glycopolymer modification could enhance intercellular adhesion between DCs and T cells. For this purpose, T cells were isolated from splenocytes using the untouched $CD3^+$ T cell isolation kit, and subsequently co-incubated with G-DCVs at a ratio of 10:1 (T cells: DCs). The binding between T cells and DCs was video-recorded every 2 minutes for 2 hours (**Figure 3A**). T cells and DCs could be easily distinguished by size and morphology, and intercellular adhesion was considered to occur when two cells remained in contact for over 2 minutes. After incubating G-DCV displaying a series of glycopolymer densities on themselves with T cells, we found that the adhesion between DCs and T cells increased with the increasing density of glycopolymers on DCs, and would reach a plateau (**Figure S11**).

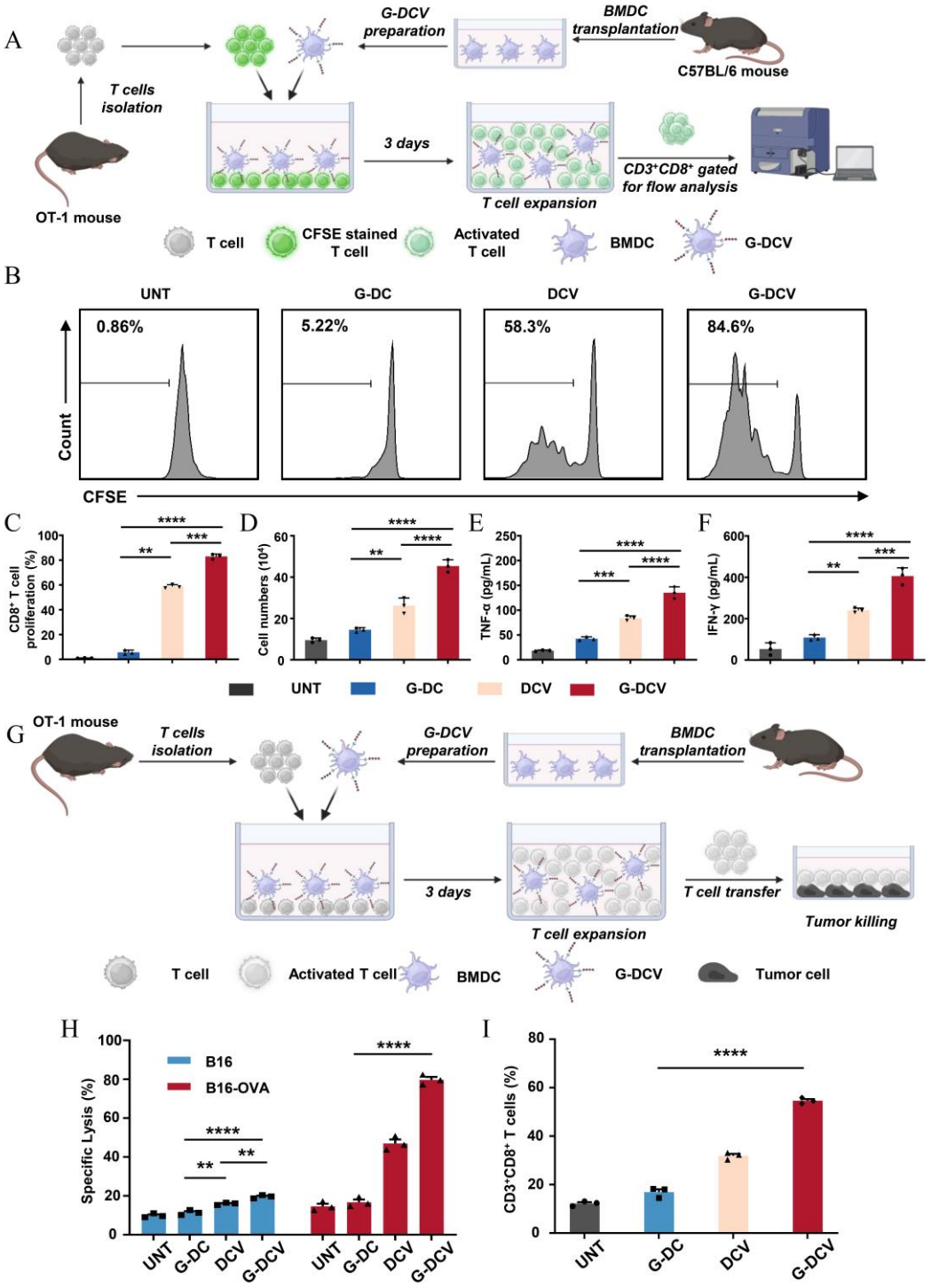

Figure 4. ***Ex vivo*** **antigen-specific T cell activation by G-DCV.** (A) Schematic diagram of the experimental procedures for verifying the ability of G-DCV to expand antigen-specific T cells *ex vivo*; (B) Flow cytometry data of $CD8^+$ T cell proliferation under various treatments, as indicated by CFSE dilution; (C) Statistic data corresponding to the flow cytometry data in (B); (D) Cell counts following incubation with BMDCs under various treatments; (E) TNF-α and (F) IFN-γ levels in the

cell culture supernatants from various treatment groups; (G) Schematic diagram of the experimental procedures showing the antigen-specific T cell activation by G-DCV for *ex vivo* targeted tumor cell killing; (H) The lysis efficacies of B16-OVA cells and B16 cells by OT-1 mouse T cells under various treatments, were examined with a 50:1 ratio of stimulated T cells and tumor cells; (I) Statistical data showing the percentage of $CD3^+CD8^+$ T cells in the T cells from various treatment groups. UNT: untreated immature BMDCs; G-DC: immature BMDCs modified with glycopolymers; DCV: mature BMDCs; G-DCV: mature BMDCs modified with glycopolymers. UNT: untreated immature BMDCs; DCV: mature BMDCs; DCV+G: mature BMDCs and free glycopolymers in the cell culture medium; G-DCV+G: mature BMDCs modified with glycopolymers and free glycopolymers in the cell culture medium; G-DCV: mature BMDCs modified with glycopolymers. The error bars represent mean ± SD (n = 3). Statistical analysis was performed using Tukey's multiple comparison test and, **p < 0.01, ***p< 0.001, ****p < 0.0001.

Next, we compared the differences in adhesion between G-DCVs and DCVs with T cells. Here, the density of glycopolymers on DCs in G-DCVs was maintained at the highest achievable value. Notably, we observed a significant increase in the number of T cells adhered to G-DCs, compared to that between T cells and unmodified DCs (**Figure 3B**). Statistical data showed that the frequency of contact between T cells and G-DCs was increased to approximately 2.4-fold compared to that between T cells and unmodified DCs (**Figure 3C**). In addition, the average adhesion time between DCs and T cells was 11 minutes, whereas it reached 42 minutes for G-DCs and T cells (**Figure 3D**). Meanwhile, free glycopolymers could not enhance the adhesion between DCs and T cells (**Figure 3B-D**), further demonstrating that the surface anchoring of glycopolymers on DCs is necessary to enhance their adhesion with T cells. We then investigated the adhesion behavior between G-DCV and T cells in the presence of excess free glycopolymers, aiming to explore whether the enhanced adhesion was due to the binding between glycopolymers and their receptors on T cells. The results demonstrated that the adhesion between DCs and T cells could not be enhanced after blocking the surface receptors of T cells with an excess of free glycopolymers (**Figure 3B-D**). Therefore, we inferred that the enhanced adhesion between DCs and T cells could be attributed to the specific or non-specific interactions between glycopolymers and some receptors on the surface of T cells. However, many receptors on T cells might have interactions with glycopolymers. To our knowledge, receptors on T cells that might bind to glycopolymers include mannose-6-phosphate receptor (M6PR)[17], natural killer cell-associated receptors (NKRs) family[18], NK-like C-type lectin-like receptor (NKCL)[19], sialic acid-binding immunoglobulin-like lectins (Siglecs) family[20], and so on. Further specialized studies including gene silencing, are needed to determine which receptors are involved in the binding of glycopolymers.

Ex Vivo Antigen-Specific T Cell Activation by G-DCV

Furthermore, we assessed the ability of G-DCV to activate antigen-specific T-cell *ex vivo* with flow cytometry-based carboxyfluorescein diacetate succinimidyl ester (CFSE) dilution assay. As mentioned above, OVA was employed as the model antigen for DCV preparation. Therefore, T cells isolated from OT-1 mice, whose $CD8^+$ T cells could specifically recognize $OVA_{257-264}$ peptides in complex with major histocompatibility complex class I (MHC-I) molecules, were utilized to validate the potential of G-DCV in expanding antigen-specific T cells. After staining with CFSE, T cells derived from OT-1 mice were co-cultured with G-DCV for 72 hours, as depicted in **Figure 4A**. Following co-culture, PerCP-labeled CD8a antibodies and PE-labeled CD3 antibodies were utilized to mark $CD8^+$ T cells to assess their proliferation with flow cytometry. We firstly explored the impact of cell surface glycopolymer densities on the T cell activation ability of G-DCV. The flow cytometry results indicated that the proliferation of $CD8^+$ T cells increased with the rise in glycopolymer density, eventually reaching a plateau, consistent with the results of the intercellular adhesion assay described above **(Figure S12**). Afterward, flow cytometry results demonstrated that G-DCV with attainable maximum glycopolymer density could more efficiently stimulate the proliferation of $CD8^+$ T cells compared to unmodified DCV. In addition, glycopolymer-modified immature DCs had little effect on T cell activation (**Figure 4B, C**). Cell counts using a cell counter yielded consistent results (**Figure 4D**). Furthermore, it was found that in the presence of free glycopolymers, the G-DCV showed a similar ability to unmodified DCV in stimulating $CD8^+$ T cell proliferation (**Figure S13**).

Additionally, we measured the concentrations of inflammatory cytokines, including tumor necrosis factor α (TNF-α) and interferon γ (IFN-γ), secreted by T cells into the cell culture supernatant using enzyme-linked immunosorbent assay (ELISA). Consistent with the flow cytometry results, T cells incubated with G-DCV were found to secrete significantly higher levels of inflammatory cytokines (TNF-α and IFN-γ) compared to those incubated with unmodified DCV (**Figure 4E, F**). Therefore, in conjunction with the aforementioned cell image tracking experiments, we deduced that the augmented T cell activation effect of G-DCV was attributed to the glycopolymer-modification which facilitated the DC-T cell adhesion.

Next, we verified the cytotoxicity of antigen-specific T cells expanded by G-DCV against tumor cells expressing corresponding antigens. Firstly, T cells from OT-1 mice were co-cultured with G-DCV for 72 hours. Then the activated T cells were incubated with B16-OVA cells or B16 cells at a ratio of 50:1 (**Figure 4G**). The cytotoxicity towards tumor cells was assessed by measuring lactate dehydrogenase (LDH) release in the culture medium. The results indicated that T cells activated by G-DCV could more effectively kill B16-OVA tumor cells compared with those stimulated by unmodified DCV (**Figure 4H**). In parallel, the activated T cells demonstrated less effectiveness in killing B16 cells that did not express the OVA antigen (**Figure 4H**). In addition, the concentrations of granzyme B and perforin in the cell culture supernatant were measured using ELISA. The results showed that apparent upregulation of granzyme B and perforin was observed upon T cells stimulated with G-DCV, when compared to those incubated with unmodified DCV (**Figure S14**). Flow cytometry results also showed that the proportion of $CD8^+$ T cells in the T cells activated by G-DCV was the highest, while DCV and G-DC were not able to stimulate $CD8^+$ T cells expansion as expected (**Figure 4I**). Based on the aforementioned results, it was determined that G-DCV exhibited significant advancements in *ex vivo* T cell activation, and glycopolymer modification might serve as a novel approach for potentiating DC vaccines.

10.1002/ange.202315782

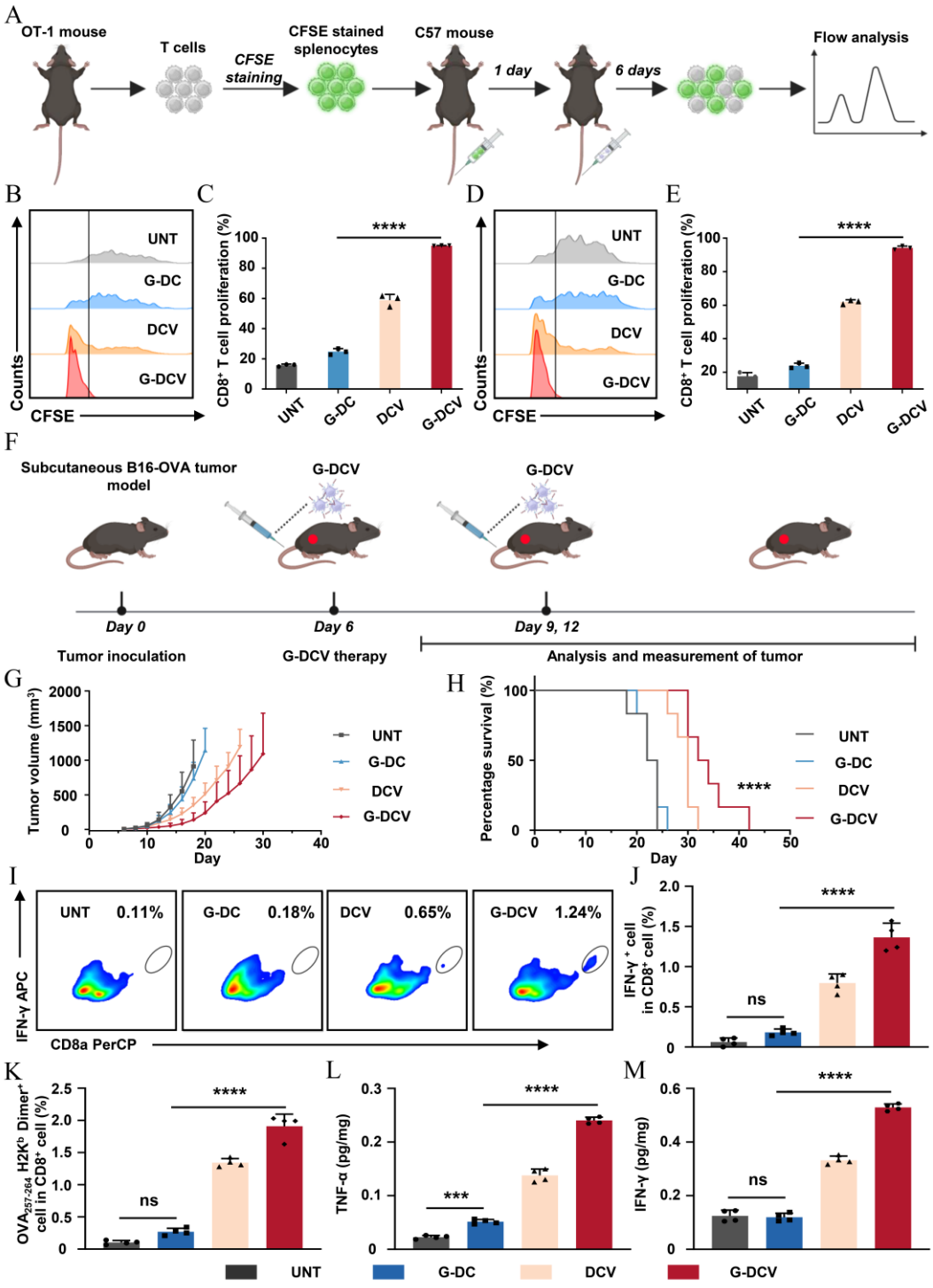

Figure 5. ***In vivo*** **antigen-specific T cell activation and B16-OVA tumor immunotherapy with G-DCV.** (A) Schematic diagram of antigen-specific T cell activation with G-DCV *in vivo*; (B) Flow cytometry data of antigen-specific T cell proliferation in the spleen under various treatments, as indicated by CFSE dilution; (C) Statistic data corresponding to the flow cytometry data in (B); (D) Flow cytometry data of antigen-specific T cell proliferation in the lymph nodes under various treatments; (E) Statistic data corresponding to the flow cytometry data in (D); (F) Schematic diagram of G-DCV to treat mouse B16-OVA tumor model; (G) Statistical tumor growth curves on B16-OVA tumor-bearing mice with various treatments as indicated (n = 6); (H) Survival rates of B16-OVA tumor-bearing mice with various treatments as indicated. Survival curves were obtained using the Kaplan–Meier method and compared by the log-rank test. ****$p < 0.0001$; (I) Representative flow cytometry data showing the proportion of IFN-γ$^+$ cells in CD8$^+$ cells in tumor tissues from different treatment groups as indicated; (J) Statistic data corresponding to the flow cytometry data in (I); (K) Statistic data of cytometry flow showing the proportion of antigen-specific T cells in CD8$^+$ cells in tumor tissues of mice under different treatments as indicated; (L) TNF-α and (M) IFN-γ levels in tumor tissues of mice under different treatments as indicated. UNT: untreated immature BMDCs; DCV: mature BMDCs; DCV+G: mature BMDCs and free glycopolymers in the cell culture medium; G-DCV+G: mature BMDCs modified with glycopolymers and free glycopolymers in the cell culture medium; G-DCV: mature BMDCs modified with glycopolymers. The error bars represent mean ± SD (n = 4). Statistical analysis was performed using Tukey's multiple comparison test and, ****$p < 0.0001$.

In Vivo Antigen-Specific T Cell Activation and Tumor Immunotherapy by G-DCV

We further investigated whether G-DCV could efficiently activate antigen-specific T cells *in vivo*. As illustrated in **Figure 5A**,

10.1002/ange.202315782

RESEARCH ARTICLE

T cells obtained from OT-1 mice were stained with CFSE, and then infused into female C57BL/6 mice via tail vein. Subsequently, G-DCV was prepared as described above and infused into the mice one day later. After 7 days, the mice were euthanized to obtain single-cell suspensions of spleen and lymph nodes to analyze the proliferation of CFSE-stained $CD8^+$ T cells. The flow cytometry results showed that antigen-specific $CD8^+$ T cells were activated more effectively both in lymph nodes (**Figure 5B, C**) and spleen (**Figure 5D, E**) by G-DC. Then, as a proof of concept, we employed G-DCV for *in vivo* immunotherapy on mice B16-OVA tumor model (a mouse melanoma model expressing the OVA antigen). On the 6th day after subcutaneous inoculation of B16-OVA tumors, mice were randomly divided into four groups: (1) untreated; (2) treated by immature BMDCs modified with glycopolymer (G-DC); (3) treated by DCV; (4) treated by G-DCV. On the 6th, 9th, and 12th day after the tumor inoculation, the G-DCV was injected into the mice, and tumor volumes and body weights of the mice were measured every two days (**Figure 5F**). The results showed that G-DCV treatment significantly inhibited tumor growth and prolonged mouse survival, whereas G-DC or DCV treatment did not yield the same effects (**Figure 5G, H**). Additionally, there were no significant alterations in the body weights of the mice compared to the control groups (**Figure S17**). Thus, we demonstrated that the glycopolymer modification could enhance the therapeutic efficacy of DCV against B16-OVA tumors.

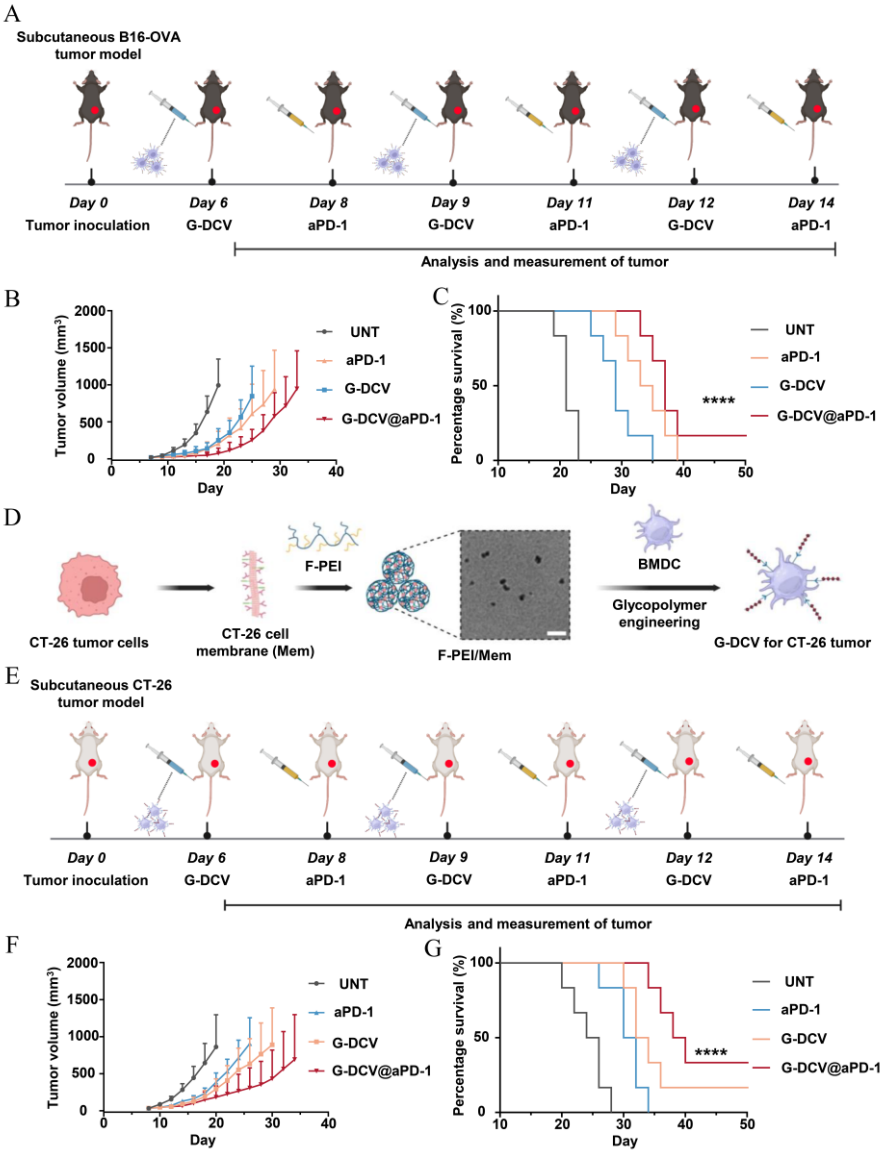

Figure 6. Tumor immunotherapy combined with G-DCV and aPD-1 in the B16-OVA and CT-26 tumor models. (A) Schematic diagram of G-DCV combined with aPD-1 to treat mouse B16-OVA tumor model; (B) Statistical tumor growth curves on B16-OVA tumor-bearing mice with various treatments as indicated; (C) Survival rates of B16-OVA tumor-bearing mice with various treatments as indicated; (D) Schematic diagram of the preparation process for constructing G-DCV for the CT-26 tumor; (E) Schematic diagram of G-DCV combined with aPD-1 to treat mouse CT-26 tumor model; (F) Schematic diagram of G-DCV combined with aPD-1 to treat mouse CT-26 tumor model; (G) Survival rates of CT-26 tumor-bearing mice with various treatments as indicated. Survival curves were obtained using the Kaplan–Meier method and compared by the log-rank test. ****$p < 0.0001$. The error bars represent mean ± SD ($n = 6$).

Subsequently, we explored the reasons behind the superior therapeutic effect of G-DCV. For this purpose, the tumor immunotherapy experiment was performed again, and the mice were euthanized to obtain tumor tissues to prepare single-cell

suspensions for flow analysis. It was found that G-DCV could increase the ratio of IFN-γ$^+$CD8$^+$ as well as OVA$_{257-246}$ H2k^b Dimer$^+$CD8$^+$ cells in tumors, indicating effective infiltration of CD8$^+$ T cells in tumor tissues (**Figure 5I-K**). Additionally, the levels of inflammatory cytokines such as TNF-α and IFN-γ in tumor tissues were also evaluated via ELISA. The concentrations of TNF-α and IFN-γ in tumor tissues were significantly enhanced by G-DCV which was beneficial to resulting in the superior tumor therapeutic outcome (**Figure 5L, M**).

Tumor Immunotherapy by G-DCV Combined with Immune Checkpoint Blockade Therapy

Tumor-mediated immunosuppression is one of the major barriers to the success of DC vaccines[6]. In recent years, the field of immune checkpoint inhibition therapy has witnessed significant advancements in its ability to reverse the suppressive tumor immune microenvironment[21]. Therefore, we further evaluated the efficacy of G-DCV in combination with immune checkpoint blockade inhibitors (PD-1 antibody, aPD-1, a commonly used immune checkpoint inhibitor) in mouse B16-OVA and CT-26 tumor models. The B16-OVA model was established as the previous approach, and the tumor-bearing mice were randomly divided into four groups: (1) untreated; (2) aPD-1 treatment; (3) G-DCV treatment; (4) G-DCV@aPD-1 treatment (**Figure 6A**). Subsequently, the G-DCV was injected on the 6th, 9th, and 12th day after tumor inoculation. On the 8th, 11th, and 14th day, aPD-1, at a dose of 10 μg per mouse was intravenously injected. The results showed that G-DCV combined with aPD-1 could more effectively inhibit tumor growth as well as prolong the survival time of mice (**Figure 6B, C**), compared with the G-DCV or aPD-1 treatment alone. Meanwhile, there was no significant change observed in the body weight of mice compared to the control groups (**Figure S19**). In addition, we evaluated the efficacy of G-DCV in combination with aPD-1 in the CT-26 tumor model. The G-DCV for the CT-26 tumor was prepared as depicted in **Figure 6D** according to the reported method previously[5c]. CT-26 cell membrane was prepared by mechanical disruption and was utilized as the antigen to replace OVA. G-DCV combined with aPD-1 could also significantly inhibit tumor growth and prolong animal survival compared to G-DCV alone or aPD-1 alone (**Figure 6E-G**). Also, there were no significant changes in body weight of the mice (**Figure S21**). The above results suggested that immune checkpoint inhibitors can further enhance the effectiveness of the G-DCV.

Conclusion

In summary, live cell surface glycopolymer engineering with metabolic sugar engineering and copper-free click-chemistry was employed to promote the adhesion between DCs and T cells, thereby improving the therapeutic efficacy of the DC vaccines in tumor immunotherapy. The enhanced adhesions between G-DCV and T cells were revealed by cell image tracking in terms of duration and frequency of contacts, which is beneficial for the antigen presentation and further activation of T cells. The results demonstrated that G-DCV could efficiently inhibit the tumor growth of the B16-OVA tumor-bearing mice and the therapeutic efficacy was further improved when combined with immune checkpoint blockade inhibitors. Thus, the present research proved that the glycopolymers-engineering strategy may become a potent strategy for designing dendritic cell-based therapeutics, and the G-DCV holds great potential in tumor immunotherapy.

Acknowledgments

This work was supported by the National Natural Science Foundation of China (21935008, T2321005, 52032008, 22277071), the National Key Research and Development Program of China (2022YFB3808200, 2021YFF0701800). Z Liu acknowledges the Xplorer Prize for support. We thank G. Chen for the valuable advice. The authors also thank the website of app.Biorender.com for the assistance in creating the illustration figures.

Keywords: cell surface modification • dendritic cell vaccines • T-cell activation • polymer • tumor immunotherapy

[1] a)R. L. Sabado, S. Balan, N. Bhardwaj, *Cell Research* **2017**, *27*, 74-95; b)Y. Wang, Y. Xiang, V. W. Xin, X.-W. Wang, X.-C. Peng, X.-Q. Liu, D. Wang, N. Li, J.-T. Cheng, Y.-N. Lyv, S.-Z. Cui, Z. Ma, Q. Zhang, H.-W. Xin, *Journal of Hematology & Oncology* **2020**, *13*, 107.

[2] a)M. Saxena, S. Balan, V. Roudko, N. Bhardwaj, *Nat Biomed Eng* **2018**, *2*, 341-346; b)W. Huo, X. Yang, B. Wang, L. Cao, Z. Fang, Z. Li, H. Liu, X. J. Liang, J. Zhang, Y. Jin, *Biomaterials* **2022**, *288*, 121722; c)A. Harari, M. Graciotti, M. Bassani-Sternberg, L. E. Kandalaft, *Nature Reviews Drug Discovery* **2020**, *19*, 635-652; d)C. Zhang, Z. Zeng, D. Cui, S. He, Y. Jiang, J. Li, J. Huang, K. Pu, *Nature Communications* **2021**, *12*, 2934; e)S. He, J. Yu, M. Xu, C. Zhang, C. Xu, P. Cheng, K. Pu, *Angewandte Chemie International Edition* **2023**, *62*, e202310178.

[3] a)S. Anguille, E. L. Smits, E. Lion, V. F. van Tendeloo, Z. N. Berneman, *Lancet Oncol* **2014**, *15*, e257-267; b)J. Constantino, C. Gomes, A. Falcao, M. T. Cruz, B. M. Neves, *Transl Res* **2016**, *168*, 74-95; c)A. D. Garg, P. G. Coulie, B. J. Van den Eynde, P. Agostinis, *Trends Immunol* **2017**, *38*, 577-593; d)H. Dong, Q. Li, Y. Zhang, M. Ding, Z. Teng, Y. Mou, *Advanced Science* **2023**, e2301339.

[4] a)J. E. Smith-Garvin, G. A. Koretzky, M. S. Jordan, *Annual Review of Immunology* **2009**, *27*, 591-619; b)H. Yang, L. Sun, R. Chen, Z. Xiong, W. Yu, Z. Liu, H. Chen, *Biomaterials* **2023**, *296*, 122048.

[5] a)K. Birkholz, M. Schwenkert, C. Kellner, S. Gross, G. Fey, B. Schuler-Thurner, G. Schuler, N. Schaft, J. Dörrie, *Blood* **2010**, *116*, 2277-2285; b)M. V. Dhodapkar, M. Sznol, B. Zhao, D. Wang, R. D. Carvajal, M. L. Keohan, E. Chuang, R. E. Sanborn, J. Lutzky, J. Powderly, H. Kluger, S. Tejwani, J. Green, V. Ramakrishna, A. Crocker, L. Vitale, M. Yellin, T. Davis, T. Keler, *Science Translational Medicine* **2014**, *6*, 232ra251; c)J. Xu, J. Lv, Q. Zhuang, Z. Yang, Z. Cao, L. Xu, P. Pei, C. Wang, H. Wu, Z. Dong, Y. Chao, C. Wang, K. Yang, R. Peng, Y. Cheng, Z. Liu, *Nat Nanotechnol* **2020**, *15*, 1043-1052; d)E. L. Dane, A. Belessiotis-Richards, C. Backlund, J. Wang, K. Hidaka, L. E. Milling, S. Bhagchandani, M. B. Melo, S. Wu, N. Li, N. Donahue, K. Ni, L. Ma, M. Okaniwa, M. M. Stevens, A. Alexander-Katz, D. J. Irvine, *Nature Materials* **2022**, *21*, 710-720; e)M. L. Bookstaver, Q. Zeng, R. S. Oakes, S. M. Kapnick, V. Saxena, C. Edwards, N. Venkataraman, S. K. Black, X. Zeng, E. Froimchuk, T. Gebhardt, J. S. Bromberg, C. M. Jewell, *Advanced Science* **2023**, *10*, 2202393; f)X. Zhang, B. Yang, Q. Ni, X. Chen, *Chemical Society Reviews* **2023**, *52*, 2886-2910.

[6] E. Garcia, S. Ismail, *International Journal of Molecular Sciences* **2020**, *21*, 3283.

10.1002/ange.202315782

[7] a)L. Zhu, R. Feng, G. Chen, C. Wang, Z. Liu, Z. Zhang, H. Chen, *ACS Applied Materials & Interfaces* **2022**, *14*, 4921-4930; b)C. Y. Lo, A. Antonopoulos, A. Dell, S. M. Haslam, T. Lee, S. Neelamegham, *Biomaterials* **2013**, *34*, 8213-8222; c)D. Sarkar, P. K. Vemula, W. Zhao, A. Gupta, R. Karnik, J. M. Karp, *Biomaterials* **2010**, *31*, 5266-5274; d)L. Yu, R. Feng, L. Zhu, Q. Hao, J. Chu, Y. Gu, Y. Luo, Z. Zhang, G. Chen, H. Chen, *Science Advances* **2020**, *6*, eabb6595.

[8] Q. Liu, S. Jiang, B. Liu, Y. Yu, Z.-A. Zhao, C. Wang, Z. Liu, G. Chen, H. Chen, *ACS Macro Letters* **2019**, *8*, 337-344.

[9] a)C. A. Hoelzel, X. Zhang, *ChemBioChem* **2020**, *21*, 1935-1946; b)X. Tang, P. Zhao, X. Wen, C. Lin, *Journal of Controlled Release* **2015**, *213*, e17-e18; c)J. Wang, K.-F. Ren, Y.-F. Gao, H. Zhang, W.-P. Huang, H.-L. Qian, Z.-K. Xu, J. Ji, *ACS Applied Bio Materials* **2019**, *2*, 2676-2684; d)H. Tang, J. Wang, L. Yu, S. Zhang, H. Yang, X. Li, J. L. Brash, L. Wang, H. Chen, *ACS Applied Materials & Interfaces* **2021**, *13*, 12594-12602.

[10] a)C. Agatemor, M. J. Buettner, R. Ariss, K. Muthiah, C. T. Saeui, K. J. Yarema, *Nature Reviews Chemistry* **2019**, *3*, 605-620; b)N. Gong, X. Han, L. Xue, R. El-Mayta, A. E. Metzloff, M. M. Billingsley, A. G. Hamilton, M. J. Mitchell, *Nature Materials* **2023**, doi: 10.1038/s41563-023-01646-6; c)H. Wang, M. C. Sobral, D. K. Y. Zhang, A. N. Cartwright, A. W. Li, M. O. Dellacherie, C. M. Tringides, S. T. Koshy, K. W. Wucherpfennig, D. J. Mooney, *Nature Materials* **2020**, *19*, 1244-1252; d)M. Hao, S. Hou, W. Li, K. Li, L. Xue, Q. Hu, L. Zhu, Y. Chen, H. Sun, C. Ju, C. Zhang, *Science Translational Medicine* **2020**, *12*, eaaz6667.

[11] a)D. Wu, K. Yang, Z. Zhang, Y. Feng, L. Rao, X. Chen, G. Yu, *Chemical Society Reviews* **2022**, *51*, 1336-1376; b)H. Yang, L. Yao, Y. Wang, G. Chen, H. Chen, *Chemical Science* **2023,** doi: 10.1039/D3SC04597H.

[12] J. Nam, S. Son, K. S. Park, J. J. Moon, *Advanced Science* **2021**, *8*, 2002577.

[13] S. R. S. Ting, E. H. Min, P. B. Zetterlund, M. H. Stenzel, *Macromolecules* **2010**, *43*, 5211-5221.

[14] M. Diehn, A. A. Alizadeh, O. J. Rando, C. L. Liu, K. Stankunas, D. Botstein, G. R. Crabtree, P. O. Brown, *Proceedings of the National Academy of Sciences* **2002**, *99*, 11796-11801.

[15] a)C. Pan, L. Wang, M. Zhang, J. Li, J. Liu, J. Liu, *Journal of the American Chemical Society* **2023**, *145*, 13261-13272; b)H. Jiang, R. Liu, L. Wang, X. Wang, M. Zhang, S. Lin, Z. Cao, F. Wu, Y. Liu, J. Liu, *Advanced Materials* **2023**, *35*, 2208157.

[16] a)J. Han, R. Bhatta, Y. Liu, Y. Bo, A. Elosegui-Artola, H. Wang, *Nature Communications* **2023**, *14*, 5049; b)X. Heng, R. Feng, L. Zhu, L. Yu, G. Chen, H. Chen, *Chinese Chemical Letters* **2022**, *33*, 4331-4334.

[17] a)A. Ara, K. A. Ahmed, J. Xiang, *Cellular & Molecular Immunology* **2018**, *15*, 986-988; b)E. J. Hindmarsh, M. A. Staykova, D. O. Willenborg, C. R. Parish, *Immunology & Cell Biology* **2001**, *79*, 436-443.

[18] E. Vivier, N. Anfossi, *Nature Reviews Immunology* **2004**, *4*, 190-198.

[19] E. Pyż, A. S. J. Marshall, S. Gordon, G. D. Brown, *Annals of Medicine* **2006**, *38*, 242-251.

[20] P. R. Crocker, J. C. Paulson, A. Varki, *Nature Reviews Immunology* **2007**, *7*, 255-266.

[21] a)M. J. Butte, M. E. Keir, T. B. Phamduy, A. H. Sharpe, G. J. Freeman, *Immunity* **2007**, *27*, 111-122; b)S. M. Ansell, A. M. Lesokhin, I. Borrello, A. Halwani, E. C. Scott, M. Gutierrez, S. J. Schuster, M. M. Millenson, D. Cattry, G. J. Freeman, S. J. Rodig, B. Chapuy, A. H. Ligon, L. Zhu, J. F. Grosso, S. Y. Kim, J. M. Timmerman, M. A. Shipp, P. Armand, *New England Journal of Medicine* **2014**, *372*, 311-319; c)Y. Chao, L. Xu, C. Liang, L. Feng, J. Xu, Z. Dong, L. Tian, X. Yi, K. Yang, Z. Liu, *Nature Biomedical Engineering* **2018**, *2*, 611-621; d)B. Li, T. Fang, Y. Li, T. Xue, Z. Zhang, L. Li, F. Meng, J. Wang, L. Hou, X. Liang, X. Zhang, Z. Gu, *Nano Today* **2022**, *46*, 101606.

10.1002/ange.202315782

WILEY VCH

RESEARCH ARTICLE

Entry for the Table of Contents

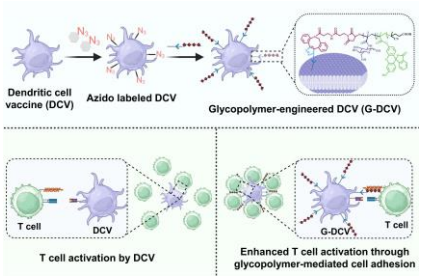

Click-chemistry-mediated cell membrane glycopolymer engineering is used to potentiate dendritic cell vaccines (DCV). The glycopolymer-engineering facilitates the adhesion of dendritic cells to T cells, thereby augmenting T cell activation and improving tumor immunotherapy, providing a new strategy for designing enhanced dendritic cell-based therapeutics.